Cylindrical and spherical modified Gardner solitons in five component dusty plasmas

Cite as: AIP Advances 13, 025356 (2023); doi: 10.1063/5.0134642
Submitted: 12 November 2022 • Accepted: 20 January 2023 •
Published Online: 23 February 2023

View Online Export Citation CrossMark

N. Y. Tanisha,[1,2,a] M. Ferdousi,[3] and K. Hossain[1]

AFFILIATIONS

[1] Department of Physics, Uttara University, Dhaka 1230, Bangladesh
[2] Department of Physics, Jahangirnagar University, Savar, Dhaka 1342, Bangladesh
[3] Nuclear Safety, Security and Safeguard Division, Bangladesh Atomic Energy Regulatory Authority, Dhaka 1207, Bangladesh

[a] Author to whom correspondence should be addressed: tanisha.90@uttarauniversity.edu.bd

ABSTRACT

The propagation of nonplanar (cylindrical or spherical) Gardner solitons (GSs) in a plasma system containing nonthermally distributed heavy ions, light ions, q nonextensive distributed electrons, and arbitrarily charged dusts is studied theoretically and numerically. The modified Gardner equation is derived using the reductive perturbation method. The basic properties (amplitude, polarity, speed, and so on) of nonplanar dust-acoustic Gardner solitons (DA GSs) are analyzed numerically. Numerical analysis shows that the properties of the DA GSs in cylindrical and spherical geometry differ from those in planar geometry. The findings of the present study considerably contribute to space plasma and laboratory plasma.

© 2023 Author(s). All article content, except where otherwise noted, is licensed under a Creative Commons Attribution (CC BY) license (http://creativecommons.org/licenses/by/4.0/). https://doi.org/10.1063/5.0134642

I. INTRODUCTION

In earlier years, much research was focused on nonlinear waves in dusty plasmas for positively and negatively charged dust.[1,2] The linear and nonlinear aspects of dust-ion-acoustic (DIA) and dust-acoustic (DA) waves are well understood in both theoretical[3–6] and experimental perspectives.[3–5] A large number of theoretical[7–9] and experimental[4,5] works were carried out by many researchers, which are valid for either Maxwellian ions or nonthermal ions at the same temperature. It is also found that ions and electrons are usually in different temperatures[10,11] in space plasma. Considering this realistic situation, the dusty plasma with two-temperature ions or electrons,[12,13] which are common in space,[14–16] and laboratory plasmas[14,17] are a topic of interest.

Nonthermally distributed ions or electrons are present in the plasma under heliospheric conditions.[7] To understand nonthermal effects in outer space plasma, especially in temperatures higher than that of the Martian ionosphere,[18] the population of nonthermal particles and their distribution attracted a great deal of attention. Jilani *et al.*[19] employed nonthermal electrons to study the ion acoustic (IA) solitons in e-p-i plasma. Alinejad[20] studied DIA solitary and shock waves in dusty plasma with nonthermal electrons. Verheest *et al.*[21] studied DIA supersolitons in dusty plasmas with nonthermal electrons employing the Sagdeev pseudo potential approach. Tasnim *et al.*[22] studied the effects of nonthermal ions of distinct temperatures on DA shock waves in a dusty plasma system. Ferdousi *et al.*[23] studied DA shock excitation in depleted dusty plasmas with κ nonthermal electrons employing the reductive perturbation approach. However, all of these works[20–23] were confined to planar geometry in the plasma system. The nonplanar geometries of practical interest include capsule implosion (spherical geometry), shock barrels (cylindrical geometry), formation of a star, explosions of a supernova, etc.

The nonextensive effects in a plasma system are common in astrophysical and cosmological cases such as stellar polytropes,[24] quark-gluon plasma,[25] hadronic matter,[25] neutron stars,[26] collisionless heating plasma,[27,28] etc., as well as in research lab requirements in nano-substances, small devices, micro-configurations, etc.

Although planar and nonplanar GSs in the plasma system were the focus of previous studies,[29,30] much remains to be understood regarding the nonlinear features of nonplanar GSs in the dusty plasma system. In this paper, we explored the cylindrical and

© Author(s) 2023

spherically modified GSs in five component dusty plasma systems using the reductive perturbation method for small but finite amplitude DA waves.

The structure of the paper is organized as follows. In Sec. II, we present the governing equations for the considered plasma system. In Sec. III, we calculate the MG equation for this system by using the reductive perturbation method. Section IV presents the analytical and numerical solutions of the MG equation. Finally, in Sec. V, we summarize our results and discuss their implications.

II. GOVERNING EQUATIONS

We address nonplanar geometry (cylindrical and spherical) in five component dusty plasma systems comprising arbitrarily charged mobile dust fluid, Cairn's distributed negatively charged heavy ions, nonthermally distributed light ions of two different temperatures, and nonextensive electrons. In the steady state, we get $n_{i10} + n_{i20} + Jz_d n_{d0} = n_{h0} + n_{e0}$, where n_{i10} (n_{i20}) is the equilibrium ion density at lower (higher) temperatures, n_{h0} is the equilibrium heavy ion density, Z_d is the number of electrons and protons located on the surface of the dust grain, n_{e0} (n_{d0}) is the density of electrons (dust particles) at equilibrium, and $J = 1(-1)$ refers to the positively (negatively) charged dust. The following normalized equations can be written for nonlinear dynamics of lower frequency waves, whose phase velocity is significantly slower than that of the thermal velocity of ions and electrons but quicker than that of the thermal velocity of dust,

$$\frac{\partial n_d}{\partial t} + \frac{1}{r^\nu}\frac{\partial}{\partial r}(r^\nu n_d u_d) = 0, \tag{1}$$

$$\frac{\partial u_d}{\partial t} + u_d\frac{\partial u_d}{\partial r} = -J\frac{\partial \phi}{\partial r}, \tag{2}$$

$$\frac{1}{r^\nu}\frac{\partial}{\partial r}\left(r^\nu \frac{\partial \phi}{\partial r}\right) = -\rho, \tag{3}$$

$$\begin{aligned} -\rho = {} & \mu\{1 + (q-1)\sigma_2\phi\}^{\frac{(q+1)}{2(q-1)}} - \mu_{i1}(1 + \beta\phi + \beta\phi^2)e^{-\phi} \\ & - \mu_{i2}(1 + \beta\sigma_1\phi + \beta\sigma_1^2\phi^2)e^{-\sigma_1\phi} \\ & + \mu_h(1 + \beta\sigma_h\phi + \beta\sigma_h^2\phi^2)e^{-\sigma_h\phi} - Jn_d, \end{aligned} \tag{4}$$

where the dust particle number density n_d is normalized by n_{d0}, the dust fluid motion u_d is normalized by $C_d = (Z_d k_B T_{i1}/m_d)^{1/2}$, the electrostatic wave potential ϕ is normalized by T_{i1}/e, ρ is the normalized surface charged density,[34] and $\sigma_1 = T_{i1}/T_{i2}$, $\sigma_2 = T_{i1}/T_e$, $\sigma_h = T_h/T_e$, $\mu_{i1} = n_{i10}/Z_d n_{d0}$, $\mu_{i2} = n_{i20}/Z_d n_{d0}$, $\mu_h = n_{h0}/Z_d n_{d0}$, and $\mu = n_{e0}/Z_d n_{d0} = \mu_{i1} + \mu_{i2} - \mu_h + J$. It is noted that T_{i1}, T_{i2}, T_h, and T_e are the lower ion temperature, higher ion temperature, heavy ion temperature, and electron temperature, respectively. The time variable t is normalized by $\omega_{pd}^{-1} = (m_d/4\pi n_{d0} Z_d^2 e^2)^{1/2}$, and the space variable x is normalized by $\lambda_{Dm} = (T_{i1}/4\pi n_{d0} Z_d e^2)^{1/2}$. The number densities of two temperature nonthermal ions, n_{i1} and n_{i2}, heavy ions n_h, and electrons n_e are

$$n_{i1} = n_{i10}\left[1 + \beta\left(\frac{e\phi}{T_{i1}}\right) + \beta\left(\frac{e\phi}{T_{i1}}\right)^2\right]e^{-\left(\frac{e\phi}{T_{i1}}\right)}, \tag{5}$$

$$n_{i2} = n_{i20}\left[1 + \beta\left(\frac{e\phi}{T_{i2}}\right) + \beta\left(\frac{e\phi}{T_{i2}}\right)^2\right]e^{-\left(\frac{e\phi}{T_{i2}}\right)}, \tag{6}$$

$$n_h = n_{h0}\left[1 + \beta\left(\frac{e\phi}{T_h}\right) + \beta\left(\frac{e\phi}{T_h}\right)^2\right]e^{-\left(\frac{e\phi}{T_h}\right)}, \tag{7}$$

$$n_e = n_{e0}\left[1 + (q-1)\frac{e\phi}{T_{i1}}\right]^{\frac{q+1}{2(q-1)}}, \tag{8}$$

where $\beta = 4\alpha/(1 + 3\alpha)$ and α expresses the population of the nonthermal ions and heavy ions. The parameter q expresses the strength of nonextensivity. In the limiting case ($q \to 1$), the q distribution function reduces to the Maxwell–Boltzmann distribution, and for $q < -1$, the q-distribution is unnormalizable. The condition $q < 1$ refers to the case of superextensivity,[31] whereas the opposite condition $q > 1$ refers to the case of subextensivity.[31]

III. DERIVATION OF THE MG EQUATION

To study finite amplitude dust-acoustic Gardner solitons (DA GSs), initially, we present the stretched coordinates[32] as

$$\zeta = \varepsilon(r - V_p t), \tag{9}$$

$$\tau = \varepsilon^3 t, \tag{10}$$

where V_p is the perturbation modes phase velocity and the smallness parameter ε measures the weakness of the dispersion[29] ($0 < \varepsilon < 1$). We expand the quantities n_d, u_d, ϕ, and ρ in power series[29] of ε in Eq. (11) where M is the system parameter that represents the system's state at a given position and time. We take into account small deviations from the equilibrium position $M^{(0)}$, which is $n_d^{(0)} = 1$, $u_d^{(0)} = 0$, $\phi^{(0)} = 0$, and $\rho^{(0)} = 0$, by employing

$$M = M^{(0)} + \sum_{n=1}^{\infty} \varepsilon^n M^{(n)}. \tag{11}$$

To the lowest order in ε, Eqs. (1)–(4) provide

$$u_d^{(1)} = \frac{J}{V_p}\phi^{(1)}, \quad n_d^{(1)} = \frac{J}{V_p^2}\phi^{(1)}, \tag{12}$$

$$V_p = \frac{1}{\sqrt{\frac{1}{2}\mu\sigma_2(1+q) + t_1(\beta - 1)}}. \tag{13}$$

Equation (13) is the linear dispersion relation for DA waves, where $t_1 = (\mu_h\sigma_h - \mu_{i1} - \mu_{i2}\sigma_1)$.

We obtain a set of equations in Eqs. (14)–(17) up to a higher level of ε using the values of $n_d^{(1)}$, $u_d^{(1)}$, and V_p,

$$u_d^{(2)} = \frac{1}{2V_p^3}\phi^2 + \frac{J\phi^{(2)}}{V_p}, \tag{14}$$

$$n_d^{(2)} = \frac{3}{2V_p^4}\phi^2 + \frac{J\phi^{(2)}}{V_p^2}, \tag{15}$$

© Author(s) 2023

$$\rho^{(2)} = -\frac{1}{2}A\phi^2 = 0, \tag{16}$$

$$A = \frac{V_p^3}{2}\left[\mu_{i1} + \mu_{i2}\sigma_1^2 - \frac{1}{4}\sigma_2\mu(1+q)(3-q) - \mu_h\sigma_h^2 + \frac{3J}{V_p^4}\right]. \tag{17}$$

The solution of $A(\mu_{i1} = \mu_C) = 0$ for μ_{i1} is given by

$$\mu_C = \frac{1}{6p_1^2}\left[J(6\mu_h p_1 p_2 + \sqrt{D} - p_6) - 6\mu_{i2}p_1p_3\right], \tag{18}$$

where $D = [J(J(16 + (1+q)\sigma_2(96 - 96\beta + 8(21+q)\sigma_2 - 48(q-3)(\beta-2)\beta\sigma_2 + 24p_5(\beta-1)\sigma_2^2 + (q-3)^2(1+q)\sigma_2^3)) + 24(2(\beta-1) - (1+q)\sigma_2)(\mu_{i2}(-4(\beta-1)(\sigma_1-1)\sigma_1 + 2(1+q)(\sigma_1^2-1)\sigma_2 + p_5(\beta-1)(\sigma_1-1)\sigma_2^2) + \mu_h(-p_5(\beta-1)\sigma_2^2(\sigma_h-1) + 4(\beta-1)(\sigma_h-1)\sigma_h - 2(1+q)\sigma_2)(\sigma_h^2-1))]$, $p_1 = (2 - 2\beta + \sigma_2 + q\sigma_2)$, $p_2 = (\sigma_2 + q\sigma_2 + 2\sigma_h - 2\beta\sigma_h)$, $p_3 = (2\sigma_1 - 2\beta\sigma_1 + \sigma_2 + q\sigma_2)$, $p_4 = (12 - 12\beta + 3\sigma_2 + 7q\sigma_2)$, $p_5 = (q-3)(1+q)$, $p_6 = 4 + (1+q)\sigma_2 p_4$, and $P = (-1+\beta)$.

Equation (18) expresses the critical value of μ_{i1} (μ_{Cp} for positively charged dust and μ_{Cn} for negatively charged dust).[33] The DASWs with positive (negative) potential exist below (above) the values of μ_{Cp} and μ_{Cn}. The critical value is $\mu_{Cp} \simeq 0.08$ for $J = 1$, $\mu_{i2} = 0.5$, $\mu_h = 1.1$, $\sigma_1 = 0.1 \sim 0.3$, $\sigma_2 = 1$, $\sigma_h = 0.125$, and $\mu_{Cn} \simeq 1.58$ for $J = -1$, $\mu_{i2} = 0.8$, $\mu_h = 1.1$, $\sigma_1 = 0.1 \sim 0.3$, $\sigma_2 = 0.41$, and $\sigma_h = 0.125$.[11] We let $A = A_0$ when $\mu_{i1} \neq \mu_C$, but $\mu_{i1} \sim \mu_C$, and for μ_{i1} around its critical value (μ_C), $A = A_0$[34] can be expressed as

$$A_0 \simeq s\left(\frac{\partial A}{\partial \mu_{i1}}\right)_{\mu_{i1}=\mu_C} |\mu_{i1} - \mu_C| = c_1 s\varepsilon, \tag{19}$$

where

$$\begin{aligned} c_1 = {} & \frac{3}{2J}\mu\frac{1}{2}(1+q)^2{\sigma_2}^2 + \frac{3}{J}(1+q)\sigma_2(\beta-1) - \frac{3}{J}\mu_{i2}(1+q)\sigma_2(\beta-1) \\ & + \frac{3}{J}\mu_h(1+q)\sigma_2(\beta-1) - 3(1+q)\sigma_2(\beta-1) - \frac{6}{J}\mu_h\sigma_h(\beta-1) \\ & - \frac{3}{J}\mu_{i1}(\beta-1)^2 - \frac{6}{J}\mu_{i2}\sigma_1(\beta-1)^2 \\ & - \frac{1}{4}(1+q)(3-q)\sigma_2 + {\sigma_h}^2 - 1. \end{aligned} \tag{20}$$

In Eq. (20), $|\mu_{i1} - \mu_C|$ is a small and dimensionless parameter[34] and can be taken as the expansion parameter ε, i.e., $|\mu_{i1} - \mu_C| \simeq \varepsilon$, $s = 1$ for $\mu_{i1} > \mu_C$, and $s = -1$ for $\mu_{i1} < \mu_C$. The surface charge density $\rho^{(2)}$ can be written as

$$\varepsilon^2\rho^{(2)} \simeq -\varepsilon^3\frac{1}{2}c_1 s\psi^2. \tag{21}$$

To the next higher level in ε, we obtain a set of equations as

$$\begin{aligned} & \frac{\partial n_d^{(1)}}{\partial \tau} - V_p\frac{\partial n_d^{(3)}}{\partial \zeta} + \frac{\partial u_d^{(3)}}{\partial \zeta} + \frac{\partial}{\partial \zeta}\left(n_d^{(1)}u_d^{(2)}\right) \\ & \quad + \frac{\partial}{\partial \zeta}\left(n_d^{(2)}u_d^{(1)}\right) + \frac{\nu u_d^{(1)}}{V_p\tau} = 0, \end{aligned} \tag{22}$$

$$\frac{\partial u_d^{(1)}}{\partial \tau} - V_p\frac{\partial u_d^{(3)}}{\partial \zeta} + u_d^{(1)}\frac{\partial u_d^{(2)}}{\partial \zeta} + u_d^{(2)}\frac{\partial u_d^{(1)}}{\partial \zeta} - \frac{\nu}{V_p^3\tau}\psi + \frac{J\partial\phi^{(3)}}{\partial \zeta} = 0, \tag{23}$$

$$\begin{aligned} & \frac{\partial^2\psi}{\partial\zeta^2} + \frac{1}{2}c_1 s\psi^2 + Jn_d^{(3)} - \frac{1}{48}\mu{\sigma_2}^3 S{\phi^{(1)}}^3 - \frac{1}{4}\mu{\sigma_2}^2(5+q)(3-q)\phi^{(1)}\phi^{(2)} \\ & - \mu\sigma_2\phi^{(3)} - \frac{1}{2}(1+q)\mu\sigma_2\phi^{(3)} - \mu_h\sigma_h(\beta-1)\phi^{(3)} \\ & - \mu_h{\sigma_h}^2\phi^{(1)}\phi^{(2)}\frac{1}{2}\mu_h\sigma_h^3\beta{\phi^{(1)}}^3 + \frac{1}{6}\mu_h{\sigma_h}^3{\phi^{(1)}}^3 + \mu_{i1}(\beta-1)\phi^{(3)} \\ & + \mu_{i1}\phi^{(1)}\phi^{(2)} + \frac{1}{2}\mu_{i1}\beta{\phi^{(1)}}^3 - \frac{1}{6}\mu_{i1}{\sigma_1}^3{\phi^{(1)}}^3 + \mu_{i2}\sigma_1(\beta-1)\phi^{(3)} \\ & + \mu_{i2}{\sigma_1}^2\phi^{(1)}\phi^{(2)} + \frac{1}{2}\mu_{i1}{\sigma_1}^3\beta{\phi^{(1)}}^3 - \frac{1}{6}\mu_{i1}{\sigma_1}^3{\phi^{(1)}}^3 = 0. \end{aligned} \tag{24}$$

Now, using Eqs. (22)–(24), we get an equation of the form

$$\frac{\partial\psi}{\partial\tau} + \frac{\nu}{2\tau}\psi + c_1 sB\psi\frac{\partial\psi}{\partial\zeta} + \alpha B\psi^2\frac{\partial\psi}{\partial\zeta} + B\frac{\partial^3\psi}{\partial\zeta^3} = 0, \tag{25}$$

where

$$\begin{aligned} \alpha = {} & \frac{1}{2}\left[\frac{15}{V_p^6} - \frac{1}{8}\mu\sigma_2^3(1+q)(5-3q)(3-q) - \frac{1}{2}\mu_h{\sigma_h}^3(1-3\beta)\right. \\ & \left. + \frac{1}{2}\mu_{i1}(1-3\beta) + \frac{1}{2}\mu_{i2}{\sigma_1}^3(1-3\beta)\right], \end{aligned} \tag{26}$$

$$B = \frac{V_p^3}{2}. \tag{27}$$

Equation (25) is known as the MG equation. The change is due to the additional term $\frac{\nu}{2\tau}\psi$ that results from the nonplanar configuration. It is observed that if we ignore the term ψ^3 and set

$$c_1 sB = A = \frac{V_p^3}{2}\left[\mu_{i1} + \mu_{i2}\sigma_1^2 - \frac{1}{4}\sigma_2\mu(1+q)(3-q) - \mu_h\sigma_h^2 + \frac{3J}{V_p^4}\right], \tag{28}$$

the MG equation reduces to a modified K-dV equation using lower order stretching[29,35] coordinates as

$$\zeta = \varepsilon^{1/2}(r - V_p t), \quad \tau = \varepsilon^{3/2}t.$$

In this modified K-dV equation, the nonlinear term disappears completely at $\mu_{i1} = \mu_C$, which causes the broad enough soliton amplitude to break down the validity of the reductive perturbation method.[29] However, the derived MG equation is valid for nonplanar configuration as well as for $\mu_{i1} \simeq \mu_C$.[29]

IV. SW SOLUTION OF THE MG EQUATION

To study stationary Gardner solitons, we introduce a transformation $\xi = \zeta - U_0\tau$, which allows us to write Eq. (25) under the steady state condition as

© Author(s) 2023

$$\frac{1}{2}\left(\frac{d\psi}{d\xi}\right)^2 + V(\psi) = 0, \tag{29}$$

where the pseudo-potential $V(\psi)$ is

$$V(\psi) = -\frac{U_0}{2B}\psi^2 + \frac{c_1 s}{6}\psi^3 + \frac{\alpha}{12}\psi^4. \tag{30}$$

In Eq. (30), U_0 and B are always positive. According to Eq. (30), it is clear that

$$V(\psi)|_{\psi=0} = \left.\frac{dV(\psi)}{d\psi}\right|_{\psi=0} = 0, \tag{31}$$

$$\left.\frac{d^2V(\psi)}{d\psi^2}\right|_{\psi=0} < 0. \tag{32}$$

The conditions in Eqs. (31) and (32) imply that SW solutions of Eq. (25) exist if

$$V(\psi)|_{\psi=\psi_m} = 0. \tag{33}$$

The latter can be solved as follows:

$$U_0 = \frac{c_1 sB}{3}\psi_{m1,2} + \frac{\alpha B}{6}\psi_{m1,2}^2, \tag{34}$$

$$\psi_{m1,2} = \psi_m\left[1 \pm \sqrt{1 + \frac{U_0}{V_0}}\right], \tag{35}$$

where $\psi_m = -c_1 s/\alpha$ and $V_0 = c_1^2 s^2 B/6\alpha$. Now, using Eqs. (34) and (35) in Eq. (25), we get

$$\left(\frac{d\psi}{d\zeta}\right)^2 + \gamma\psi^2(\psi - \psi_{m1})(\psi - \psi_{m2}) = 0, \tag{36}$$

where $\gamma = \alpha/6$. The SW solution of Eq. (25) or Eq. (35) is

$$\psi = \left[\frac{1}{\psi_{m2}} - \left(\frac{1}{\psi_{m2}} - \frac{1}{\psi_{m1}}\right)\cosh^2\left(\frac{\xi}{\delta}\right)\right]^{-1}, \tag{37}$$

where the width of the MG soliton δ is

$$\delta = \frac{2}{\sqrt{-\gamma\psi_{m1}\psi_{m2}}}. \tag{38}$$

Equation (38) expresses the SW solution of Eq. (25). To find the parametric regimes where positive and negative solitary potential profiles exist, we carried out a numerical analysis and found $A(\mu_{i1} = \mu_C) = 0$ surface plots. The $A(\mu_{i1} = \mu_C) = 0$ surface plots are shown in Figs. 1 and 2. In Fig. 1, it is seen that μ_{Cp} gradually decreases with

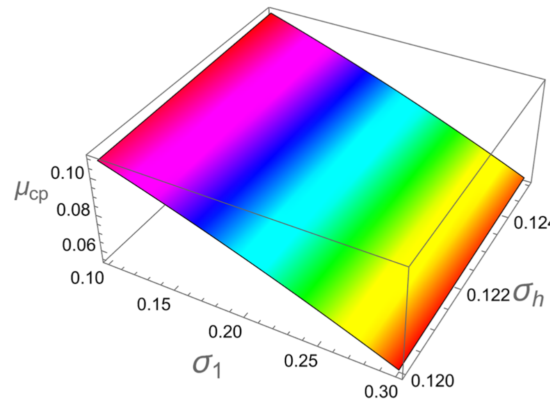

FIG. 1. Graph for $A = 0$, which shows the variation of μ_{Cp} with σ_1 and σ_h for $J = 1$, where μ_{Cp} is the critical value of μ_{i1} above or below which positive or negative potential solitons are found.

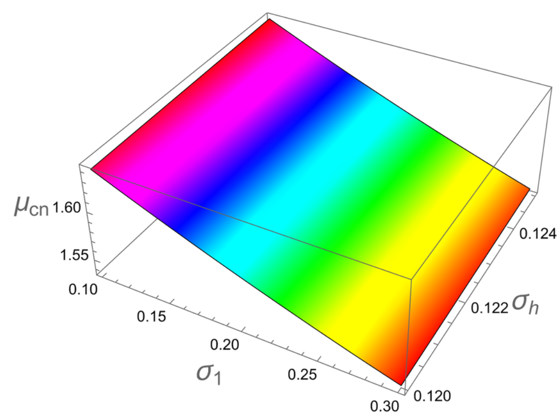

FIG. 2. Graph for $A = 0$, which shows the variation of μ_{Cn} with σ_1 and σ_h for $J = -1$, where μ_{Cn} is the critical value of μ_{i1} above or below which positive or negative potential solitons are found.

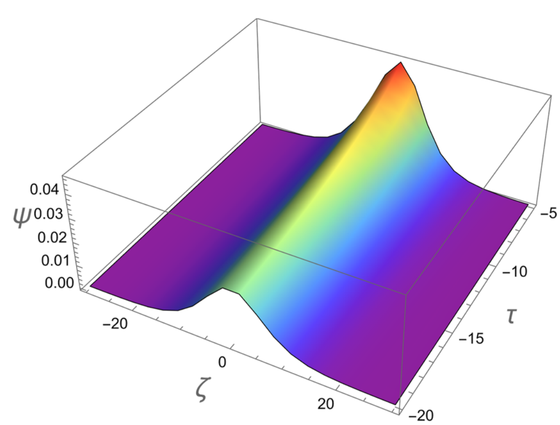

FIG. 3. Amplitude variation of positive DA GSs for cylindrical $(\nu = 1)$ configuration with $\mu_{i1} = 0.3$, $\mu_{i2} = 0.8$, $\mu_h = 1.1$, $\sigma_1 = 0.2$, $\sigma_2 = 1$, $\sigma_h = 0.125$, $\beta = 0.6$, $q = 0.3$,[33] $s = 1$, and $J = 1$, where $\mu_{i1} > \mu_{Cp}$.

© Author(s) 2023

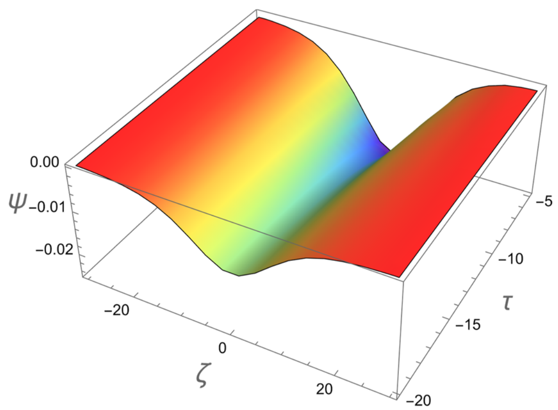

FIG. 4. Amplitude variation of negative DA GSs for cylindrical $(\nu = 1)$ configuration with $\mu_{i1} = 0.05$, $\mu_{i2} = 0.8$, $\mu_h = 1.1$, $\sigma_1 = 0.2$, $\sigma_2 = 1$, $\sigma_h = 0.125$, $\beta = 0.6$, $q = 0.3$,[33] $s = -1$, and $J = 1$, where $\mu_{i1} < \mu_{Cp}$.

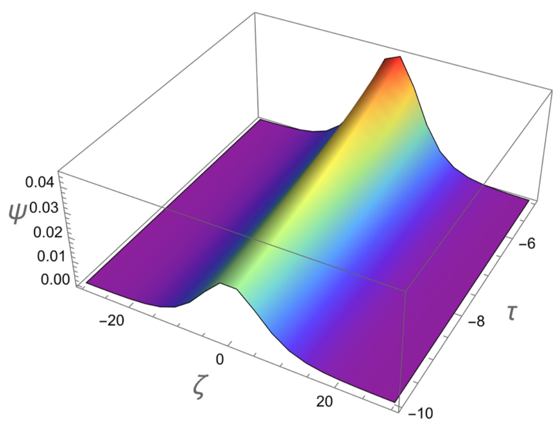

FIG. 5. Amplitude variation of positive DA GSs for spherical $(\nu = 2)$ configuration with $\mu_{i1} = 0.3$, $\mu_{i2} = 0.8$, $\mu_h = 1.1$, $\sigma_1 = 0.2$, $\sigma_2 = 1$, $\sigma_h = 0.125$, $\beta = 0.6$, $q = 0.3$,[33] $s = 1$, and $J = 1$, where $\mu_{i1} > \mu_{Cp}$.

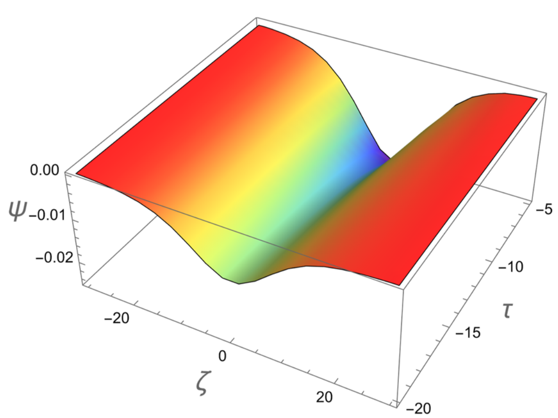

FIG. 6. Amplitude variation of negative DA GSs for spherical $(\nu = 2)$ configuration with $\mu_{i1} = 0.05$, $\mu_{i2} = 0.8$, $\mu_h = 1.1$, $\sigma_1 = 0.2$, $\sigma_2 = 1$, $\sigma_h = 0.125$, $\beta = 0.6$, $q = 0.3$,[33] $s = -1$, and $J = 1$, where $\mu_{i1} < \mu_{Cp}$.

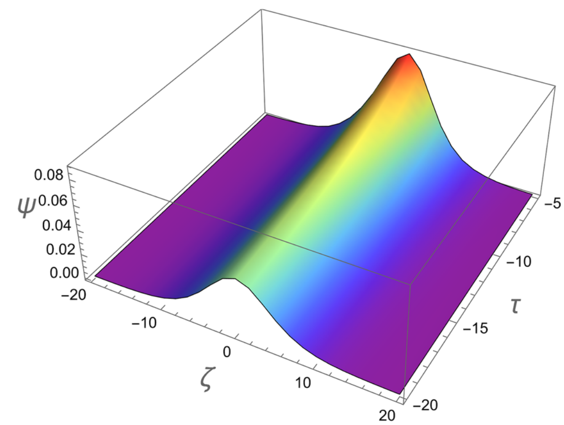

FIG. 7. Amplitude variation of positive DA GSs for cylindrical $(\nu = 1)$ configuration with $\mu_{i1} = 2.3$, $\mu_{i2} = 0.8$, $\mu_h = 1.1$, $\sigma_1 = 0.2$, $\sigma_2 = 0.41$, $\sigma_h = 0.125$, $\beta = 0.6$, $q = 0.3$,[33] $s = 1$, and $J = -1$, where $\mu_{i1} > \mu_{Cn}$.

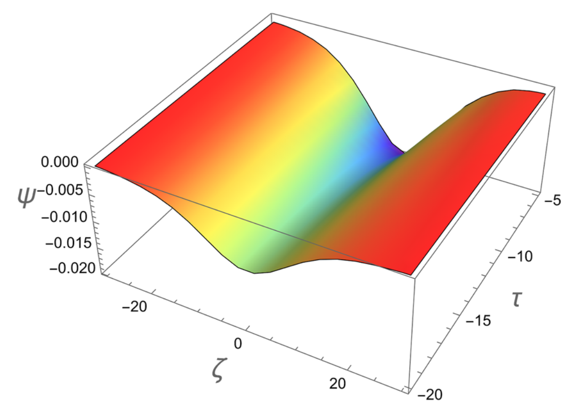

FIG. 8. Amplitude variation of negative DA GSs for cylindrical $(\nu = 1)$ configuration with $\mu_{i1} = 1.17$, $\mu_{i2} = 0.8$, $\mu_h = 1.1$, $\sigma_1 = 0.2$, $\sigma_2 = 0.41$, $\sigma_h = 0.125$, $\beta = 0.6$, $q = 0.3$,[33] $s = -1$, and $J = -1$, where $\mu_{i1} < \mu_{Cn}$.

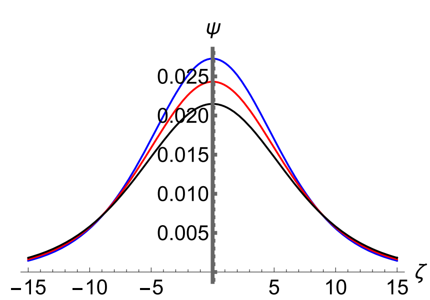

FIG. 9. Amplitude variation of positive DA GSs with β for $\mu_{i1} = 0.3$, $\mu_{i2} = 0.8$, $\mu_h = 1.1$, $\sigma_1 = 0.2$, $\sigma_2 = 1$, $\sigma_h = 0.125$, $q = 0.3$, $s = 1$, and $J = 1$, where $\mu_{i1} > \mu_{Cp}$. The blue line is for $\beta = 0.3$, the red line is for $\beta = 0.5$, and the black line is for $\beta = 0.7$.

© Author(s) 2023

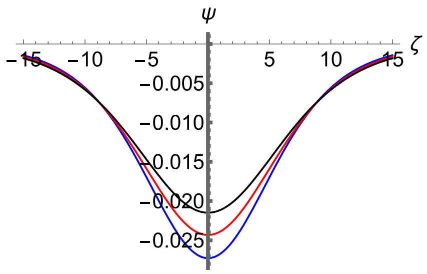

FIG. 10. Amplitude variation of negative DA GSs with β for $\mu_{i1} = 0.05$, $\mu_{i2} = 0.8$, $\mu_h = 1.1$, $\sigma_1 = 0.2$, $\sigma_2 = 1$, $\sigma_h = 0.125$, $q = 0.3$, $s = -1$, and $J = 1$, where $\mu_{i1} < \mu_{Cp}$. The blue line is for $\beta = 0.3$, the red line is for $\beta = 0.5$, and the black line is for $\beta = 0.7$.

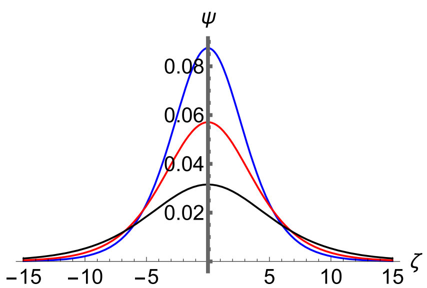

FIG. 11. Amplitude variation of positive GSs with β for $\mu_{i1} = 2.3$, $\mu_{i2} = 0.8$, $\mu_h = 1.1$, $\sigma_1 = 0.2$, $\sigma_2 = 0.41$, $\sigma_h = 0.125$, $q = 0.3$, $s = 1$, and $J = -1$, where $\mu_{i1} > \mu_{Cn}$. The blue line is for $\beta = 0.3$, the red line is for $\beta = 0.5$, and the black line is for $\beta = 0.7$.

the increase in σ_h and σ_1, and in Fig. 2, it is seen that μ_{Cn} gradually decreases with the increase in σ_h and σ_1.

In this paper, we have solved Eq. (25) numerically and studied the effects of nonplanar (spherical and cylindrical) geometries on time dependent DA GSs with nonextensive distributed electrons, nonthermally distributed ions, and heavy ions. The results are shown in Figs. 3–12. In numerical analysis, the static solution of Eq. (25) presents the initial condition without the term $\frac{\nu}{2\tau}\psi$.

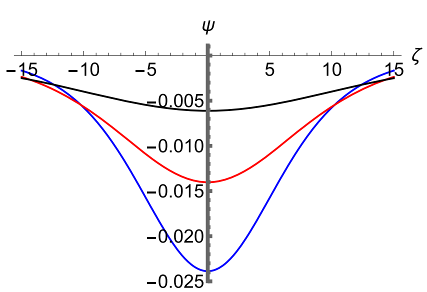

FIG. 12. Amplitude variation of negative GSs with β for $\mu_{i1} = 1.17$, $\mu_{i2} = 0.8$, $\mu_h = 1.1$, $\sigma_1 = 0.2$, $\sigma_2 = 0.41$, $\sigma_h = 0.125$, $q = 0.3$, $s = -1$, and $J = -1$, where $\mu_{i1} < \mu_{Cn}$. The blue line is for $\beta = 0.3$, the red line is for $\beta = 0.5$, and the black line is for $\beta = 0.7$.

V. SUMMARY AND DISCUSSION

We have studied an unmagnetized five-component plasma system consisting of two populations of nonthermal ions with two different temperatures, Boltzmann distributed electrons and negatively charged dust fluid. The main results are as follows:

1. The considered plasma system supports finite amplitude GSs, whose fundamental characteristics (viz., amplitude, polarity, velocity, and width) strongly depend on many plasma properties, specifically, μ_{i1}, μ_{i2}, μ_h, σ_1, σ_1, σ_2, σ_h, q, and β.
2. The fundamental characteristics of GSs exist around $\mu_{i1} = \mu_C$, and it is found that they are distinct from K-dV solitons, which do not occur at $\mu_{i1} = \mu_C$.
3. The positive GSs exist when $\mu_{i1} > \mu_{Cp}$ and negative GSs exist when $\mu_{i1} < \mu_{Cp}$ for $J = 1$.[36]
4. The positive GSs exist when $\mu_{i1} > \mu_{Cn}$ and negative GSs exist when $\mu_{i1} < \mu_{Cn}$ for $J = -1$.
5. For $J = 1$ where $\mu_{i1} > \mu_{Cp}$, the amplitude of the positive GSs decreases with the increase in β, as shown in Fig. 9, and for $J = 1$ where $\mu_{i1} < \mu_{Cp}$, the amplitude of the negative GSs increases with the increase in β, as shown in Fig. 10.
6. For $J = -1$ where $\mu_{i1} > \mu_{Cn}$, the amplitude of the positive GSs decreases with the increase in β, as shown in Fig. 11, and for $J = -1$ where $\mu_{i1} < \mu_{Cn}$, the amplitude of the negative GSs increases with the increase in β, as shown in Fig. 12.
7. Equation (25) illustrates that $\frac{\nu}{2\tau}\psi$ reaches infinity when $\tau \to 0$. As a result, this term has a singular value at $\tau = 0$. This term disappears for large values of τ, and we find the modified Gardner equation. We begin with a large value of τ such as $\tau = -5$ in the direction of time, where the term $\frac{\nu}{2\tau}\psi$ is insignificant. The importance of the nonplanar geometrical impact is clear from Eq. (25) when $\tau \to 0$, and it becomes weaker with the increase in τ.
8. According to the numerical solutions of Eq. (25), the nonplanar DA GSs are identical for higher values of τ. It is discovered that the amplitude of cylindrical 1D planar DA GSs is higher than that of 1D spherical ones and smaller than that of the spherical ones. The amplitudes of nonplanar (spherical and cylindrical) DA GSs increase when τ decreases, as shown in Figs. 3–8.

In the considered plasma system, cylindrical and spherical geometries and nonthermal effects play an important role in the basic characteristics of DA GSs, viz., amplitude, width, polarity, etc. Overall, the findings of this present study have illustrated the rich variety of nonlinear aspects of DA GSs in different outer space plasmas (viz., ionospheres,[37] auroral acceleration regions, explosions of cluster, supernovas, active galactic nuclei, pulsar environments, etc.) in addition to experimental species (viz., semiconductor plasmas[38] and intense laser fields[39]) in the principal plasma species.[40]

ACKNOWLEDGMENTS

The authors thank Dr. A. A. Mamun and Dr. S. Sultana for their guidance and encouragement.

© Author(s) 2023

AUTHOR DECLARATIONS

Conflict of Interest

The authors have no conflicts to disclose.

Author Contributions

N. Y. Tanisha: Writing – original draft (lead); Writing – review & editing (lead). **M. Ferdousi**: Writing – review & editing (lead). **K. Hossain**: Writing – review & editing (supporting).

DATA AVAILABILITY

Data sharing is not applicable to this article as no new data were created or analyzed in this study.

REFERENCES

[1] P. H. Sakanaka and P. K. Shukla, Phys. Scr. **T84**, 181 (2000).
[2] I. Spassovska and P. H. Sakanaka, AIP Conf. Proc. **784**, 506 (2005).
[3] A. Barkan, N. D'Angelo, and R. L. Merlino, Planet. Space Sci. **44**, 239 (1996).
[4] N. N. Rao, P. K. Shukla, and M. Y. Yu, Planet. Space Sci. **38**, 543 (1990).
[5] A. Barkan, R. L. Merlino, and N. D'Angelo, Phys. Plasmas **2**, 3563 (1995).
[6] T. I. Rajib, N. K. Tamanna, N. A. Chowdhury, A. Mannan, S. Sultana, and A. A. Mamun, Phys. Plasmas **26**, 123701 (2019).
[7] P. K. Shukla and A. A. Mamun, *Introduction to Dusty Plasma Physics* (Institute of Physics Publishing Ltd., Bristol, 2002).
[8] F. Verheest, *Waves in Dusty Space Plasmas* (Kluwer Academic Press, Dordrecht, 2000).
[9] P. K. Shukla and L. Stenflo, Astrophys. Space Sci. **190**, 23 (1992).
[10] T. S. Gill, H. Kaur, and N. S. Saini, J. Plasma Phys. **70**, 481 (2004).
[11] K. B. Zhang, J. Korean Phys. Soc. **55**, 1461 (2009).
[12] I. Kourakis, S. Sultana, and M. A. Hellberg, Plasma Phys. Control. Fusion **54**, 105016 (2012).
[13] S. Sultana and A. A. Mamun, Astrophys. Space Sci. **349**, 229 (2014).
[14] A. A. Mamun and P. K. Shukla, Geophys. Res. Lett. **29**, 1870, https://doi.org/10.1029/2002gl015219 (2002).
[15] N. Dubouloz, R. Pottelette, M. Malingre, and R. A. Treumann, Geophys. Res. Lett. **18**, 155, https://doi.org/10.1029/90gl02677 (1991).
[16] M. Berthomier, R. Pottelette, M. Malingre, and Y. Khotyaintsev, Phys. Plasmas **7**, 2987 (2000).
[17] H. Derfler and T. C. Simonen, Phys. Fluids **12**, 269 (1969).
[18] R. Lundin, A. Zakharov, R. Pellinen, H. Borg, B. Hultqvist, N. Pissarenko, E. M. Dubinin, S. W. Barabash, I. Liede, and H. Koskinen, Nature **341**, 609 (1989).
[19] K. Jilani, A. M. Mirza, and T. A. Khan, Astrophys. Space Sci. **344**, 135 (2012).
[20] H. Alinejad, Astrophys. Space Sci. **327**, 131 (2010).
[21] F. Verheest, M. A. Hellberg, and I. Kourakis, Phys. Rev. E **87**, 043107 (2013).
[22] I. Tasnim, M. M. Masud, and A. A. Mamun, Phys. Rev. A **343**, 647 (2013).
[23] M. Ferdousi, S. Sultana, M. M. Hossen, M. Rashed Miah, and A. A. Mamun, Eur. Phys. J. D **71**, 102 (2017).
[24] A. R. Plastino and A. Plastino, Phys. Lett. A **174**, 384 (1993).
[25] G. Gervino, A. Lavagno, and D. Pigato, Cent. Eur. J. Phys. **10**, 594 (2012).
[26] A. Lavagno and D. Pigato, Eur. Phys. J. A **47**, 52 (2011).
[27] J. A. S. Lima, R. Silva, and J. Santos, Phys. Rev. E **61**, 3260 (2000).
[28] H. Reza Pakzad, Phys. Scr. **83**, 015505 (2011).
[29] S. A. Ema, M. Ferdousi, and A. A. Mamun, Phys. Plasmas **22**, 043702 (2015).
[30] N. Jannat, M. Ferdousi, and A. A. Mamun, Plasma Phys. Rep. **42**, 678 (2016).
[31] A. A. Mamun, M. Ferdousi, and S. Sultana, Phys. Scr. **90**, 088011 (2015).
[32] S. Bansal, M. Aggarwal, and T. S. Gill, Phys. Plasmas **27**, 083704 (2020).
[33] N. Y. Tanisha, I. Tasnim, S. Sultana, M. Salahuddin, and A. A. Mamun, Astrophys. Space Sci. **353**, 137 (2014).
[34] I. Tasnim, M. M. Masud, M. Asaduzzaman, and A. A. Mamun, Chaos **23**, 013147 (2013).
[35] H. Demiray, E. R. El-Zahar, and S. A. Shan, TWMS J. Appl. Eng. Math. **10**, 532 (2020).
[36] M. M. Rahman, M. S. Alam, and A. A. Mamun, Astrophys. Space Sci. **352**, 193 (2014).
[37] J. Bremer, P. Hoffmann, A. H. Manson, C. E. Meek, R. Rüster, and W. Singer, Ann. Geophys. **14**, 1317 (1996).
[38] P. K. Shukla, N. N. Rao, M. Y. Yu, and N. L. Tsintsadze, Phys. Rep. **138**, 1 (1986).
[39] V. I. Berezhiani, D. D. Tskhakaya, and P. K. Shukla, Phys. Rev. A **46**, 6608 (1992).
[40] N. M. Heera, J. Akter, N. K. Tamanna, N. A. Chowdhury, T. I. Rajib, S. Sultana, and A. A. Mamun, AIP Adv. **11**, 055117 (2021).

© Author(s) 2023